368 *Inorg. Chem.* **2010**, *49*, 368–370
DOI: 10.1021/ic902052f

Inorganic Chemistry
Communication

Contrasting Magnetism of $[Mn^{III}_4]$ and $[Mn^{II}_2Mn^{III}_2]$ Squares

Takuto Matsumoto,[†] Takuya Shiga,[†] Mao Noguchi,[†] Tatsuya Onuki,[†] Graham N. Newton,[†] Norihisa Hoshino,[†] Motohiro Nakano,[‡] and Hiroki Oshio*[,†]

[†]*Graduate School of Pure and Applied Sciences, University of Tsukuba, Tennodai 1-1-1, Tsukuba 305-8571, Japan and* [‡]*Department of Applied Chemistry, Graduate School of Engineering, Osaka University, 2-1 Yamada-Oka, Suita, Osaka 565-0871, Japan*

Received October 16, 2009

Two tetranuclear manganese distorted square-shaped clusters, $[Mn^{III}_4(L1)_4(\mu_2\text{-}OMe)_4]\cdot 2.5H_2O$ (**1**) and $[Mn^{II}_2Mn^{III}_2(L2)_4(H_2O)_2](PF_6)_2\cdot CHCl_3\cdot CH_3OH\cdot 1.5H_2O$ (**2**) (H_2L1 = 2-[3-(2-hydroxyphenyl)-1*H*-pyrazol-5-yl]-6-pyridinecarboxylic acid methyl ester; H_2L2 = 2-[3-(2-hydroxyphenyl)-1*H*-pyrazol-5-yl]-6-pyridinecarboxylic acid ethyl ester), exhibit antiferromagnetic and ferromagnetic interactions between neighboring manganese ions, respectively.

Well-designed polynuclear complexes show various physical properties and functionalities because of the synergy of the interactions between metal ions.[1] Various complexes, which have regular arrays such as grids,[2] wires,[3] and rings,[4] have been prepared using a range of synthetic methods. Tetranuclear complexes with square-shaped arrangements of metal ions are of great interest to the chemist because of their potential application as molecular devices, such as quantum cellular automata.[5] The controllable arrangement of metal ions in multinuclear complexes is achieved through rational ligand design and the bonding affinities of different metal ions. Planar multidentate bridging ligands can afford $n \times n$ square gridlike complexes, such as those reported by Thompson, Lehn, and others.[2] These grid complexes were formed by spontaneous self-assembly due to the directing geometries of the ligands. Hydrazone- and polypyridyl-type ligands have been used by many researchers to construct $n \times n$ grid complexes. However, most metal ions coordinated in these complexes have octahedral coordination geometries and the same oxidation states. Thus, heterometallic gridlike complexes have been rarely reported.[6] Against such a background, the development of asymmetric planar ligands is important for the generation of novel grid-type complexes because asymmetric ligands can stabilize heterometallic and mixed-valence species. Recently, we reported the first grid-type single-molecule magnet: a $[Co_9]$ complex supported by symmetric polypyridine ligands.[2c] To develop our research further, an asymmetric planar multidentate ligand derived from 2,6-substituted pyridine was designed, and its complexation behavior has been investigated. This paper describes the syntheses, crystal structures, and magnetic properties of two tetranuclear manganese gridlike complexes, $[Mn^{III}_4(L1)_4(\mu_2\text{-}OMe)_4]\cdot 2.5H_2O$ (**1**) and $[Mn^{II}_2Mn^{III}_2(L2)_4(H_2O)_2](PF_6)_2\cdot CHCl_3\cdot CH_3OH\cdot 1.5H_2O$ (**2**) [Figure 1; H_2L1 = 2-[3-(2-hydroxyphenyl)-1*H*-pyrazol-5-yl]-6-pyridinecarboxylic acid methyl ester; H_2L2 = 2-[3-(2-hydroxyphenyl)-1*H*-pyrazol-5-yl]-6-pyridinecarboxylic acid ethyl ester (Scheme 1)].

The asymmetric multidentate ligand H_2L2 was synthesized using the Claisen condensation reaction of 2-hydroxoacetophenone with 2,6-pyridinecarboxylic acid ethyl ester.[7] The reaction of $Mn(OAc)_2\cdot 4H_2O$ with H_2L2 and Et_3N in methanol yielded the tetranuclear Mn^{III}_4 complex **1**, while the same procedure, in the presence of a stoichiometric quantity of bis(pentamethylcyclopentadienyl)iron as a reducing agent,

*To whom correspondence should be addressed. E-mail: oshio@chem.tsukuba.ac.jp.

(1) (a) Lehn, J.-M. *Supramolecular Chemistry: Concepts and Perspectives*; VCH: Weinheim, Germany, 1995. (b) Leininger, S.; Olenyuk, B.; Stang, P. J. *Chem. Rev.* **2000**, *100*, 853. (c) Fujita, M. *Chem. Soc. Rev.* **1998**, *27*, 417. (d) Gatteschi, D.; Sessoli, R.; Villain, J. *Molecular Nanomagnets*; Oxford Press: New York, 2006.

(2) (a) Thompson, L. K.; Waldmann, O.; Xu, Z. *Coord. Chem. Rev.* **2005**, *249*, 2677. (b) Ruben, M.; Rojo, J.; Romero-Salguero, F. J.; Uppadine, L. H.; Lehn, J.-M. *Angew. Chem., Int. Ed.*, **2004**, *43*, 3644 and references cited therein. (c) Shiga, T.; Matsumoto, T.; Noguchi, M.; Onuki, T.; Hoshino, N.; Newton, G. N.; Nakano, M.; Oshio, H. *Chem. Asian J.* **2009**, *4*, 1660.

(3) (a) Yin, C.; Huang, G.-C.; Kuo, C.-K.; Fu, M.-D.; Lu, H.-C; Ke, J.-H.; Shih, K.-N.; Huang, Y.-L.; Lee, G.-H.; Yeh, C.-Y.; Chen, C.-h.; Peng, S.-M. *J. Am. Chem. Soc.* **2008**, *130*, 10090. (b) Liu, I. P.-C.; Bénard, M.; Hasanov, H.; Chen, I.-W. P.; Tseng, W.-H.; Fu, M.-D.; Rohmer, M.-M.; Chen, C.-h.; Lee, G.-H.; Peng, S.-M. *Chem.—Eur. J.* **2007**, *13*, 8667. (c) Ismayilov, R. H.; Wang, W.-X.; Wang, R.-R.; Yeh, C.-Y.; Lee, G.-H.; Peng, S.-M. *Chem. Commun.* **2007**, 1121.

(4) (a) Affronte, M.; Carretta, S.; Timco, G. A.; Winpenny, R. E. P. *Chem. Commun.* **2007**, 1789. (b) Campos-Fernández, C. S.; Schottel, B. L.; Chifotides, H. T.; Bera, J. K.; Bacsa, J.; Koomen, J. M.; Russell, D. H.; Dunbar, K. R. *J. Am. Chem. Soc.* **2005**, *127*, 12909.

(5) (a) Zhao, Y.; Guo, D.; Liu, Y.; He, C.; Duan, C. *Chem. Commun.* **2008**, *44*, 5725. (b) Jiao, J.; Long, G. J.; Rebbouh, L.; Grandjean, F.; Betty, A. M.; Fehlner, T. P. *J. Am. Chem. Soc.* **2005**, *127*, 17819. (c) Lent, C. S.; Isaksan, B.; Lieberman, M. *J. Am. Chem. Soc.* **2003**, *125*, 1056. (d) Qi, H.; Sharma, S.; Li, Z.; Snider, G. L.; Orlov, A. O.; Lent, C. S.; Fehlner, T. P. *J. Am. Chem. Soc.* **2003**, *125*, 15250. (e) Lent, C. S. *Science* **2000**, *288*, 1597. (f) Imre, A.; Csaba, G.; Ji, L.; Orlov, A. O.; Bernstein, G. H.; Porod, W. *Science* **2006**, *311*, 205.

(6) (a) Petitjean, A.; Kyritsakas, N.; Lehn, J.-M. *Chem. Commun.* **2004**, 1168. (b) Parsons, S. R.; Thompson, L. K.; Dey, S. K.; Wilson, C.; Howard, J. A. K. *Inorg. Chem.* **2006**, *45*, 8832.

 Published on Web 12/14/2009

yielded a mixed-valence tetranuclear $Mn^{II}_2Mn^{III}_2$ complex, **2**.[8] During the synthesis of **1**, the ethyl ester ligand H_2L2 was transformed into the methyl ester H_2L1 by solvolysis.

X-ray structural analyses of **1** and **2** reveal that both complexes have 2 × 2 gridlike tetranuclear manganese cores bridged by the pyrazole groups of the 2,6-substituted pyridine ligands (L1 and L2).[9] **1** crystallizes in the orthorhombic space group *Pnnn*, where the asymmetric unit is half of the molecule. In **1**, each manganese ion has a square-pyramidal N_2O_3 coordination environment with two pyrazole nitrogen atoms, two oxygen atoms of μ_2-MeO^- ions, and one phenoxo oxygen atom. The pyridyl nitrogen atoms of the ligands weakly coordinate to the manganese ions, where the average distance between manganese and nitrogen atoms is 2.618 Å, suggesting axial elongation along the N6−Mn1−O8 and N3−Mn2−O7 vectors. The coordination bond lengths with equatorially coordinated atoms are in the range of 1.858−2.018 Å. The bond lengths, observed Jahn−Teller distortions, and bond valence sum (BVS) calculations[10] suggest that all manganese ions are trivalent. **2** crystallizes in the triclinic space group $P\bar{1}$. Although there are four crystallographically independent manganese ions in the complex, chemically they can be grouped into two types. The Mn1 and Mn3 ions have a square-pyramidal N_2O_3 coordination environment, coordinated by two pyrazole nitrogen atoms, two phenoxo oxygen atoms, and one oxygen atom of a water molecule, with basal coordination bond lengths in the range of 1.848−1.989 Å and axial water molecule bond lengths of 2.145(8) and 2.197(6) Å. The Mn2 and Mn4 ions have a highly distorted and elongated octahedral N_4O_2 coordination geometry with two pyridyl nitrogen atoms and two pyrazole nitrogen atoms with bond lengths in the ranges of 2.239−2.251 and 2.168−2.209 Å, respectively. The coordination environment is completed by two weakly

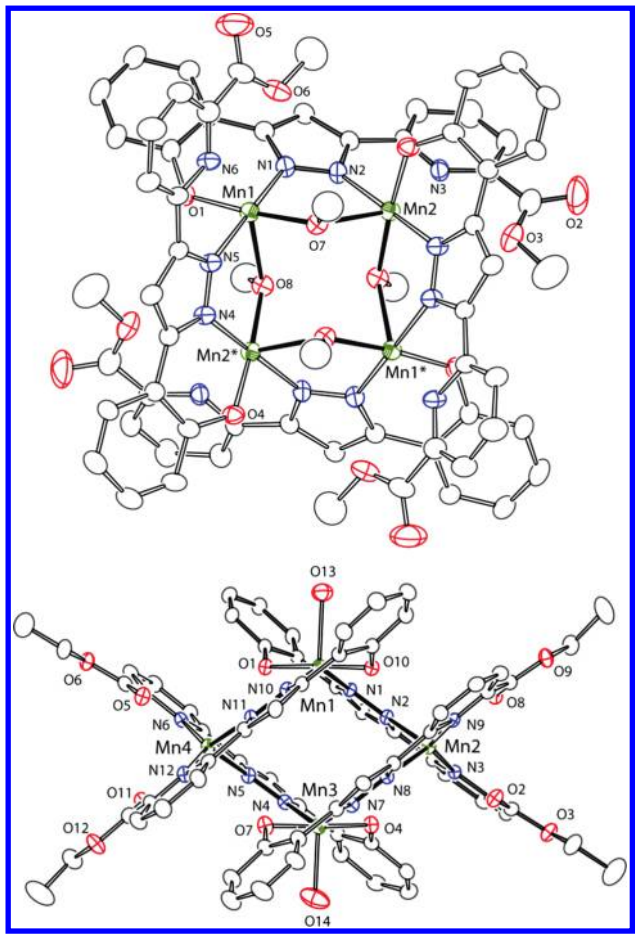

Figure 1. ORTEP diagrams of **1** (top) and **2** (bottom). Ellipsoids are at 30% probability, carbon atoms are represented by full ellipsoids, and all hydrogen atoms and solvent molecules are excluded for clarity.

Scheme 1. Ligands H_2L1 and H_2L2

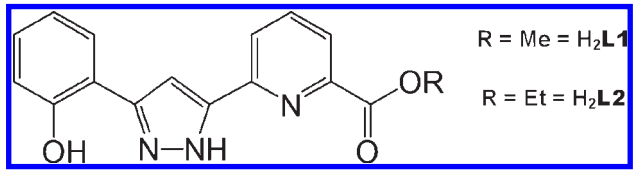

(7) Ligand synthesis. **6-[1,3-Dioxo-3-(2-hydroxyphenyl)propionyl]pyridine-2-carboxylic acid ethyl ester:** A solution of sodium ethoxide (prepared from sodium (6.99 g, 304 mmol)), acetophenone (22.88 g, 168 mmol), and 2,6-pyridinedicarboxylic acid ethyl ester (25.0 g, 112 mmol) in 100 mL of diethyl ether was refluxed for 2 h under a nitrogen atmosphere. The solvent was removed by filtration, and aqueous acetic acid (15%) was added to the residue. The resulting yellow solid was filtered, and the recrystallization of the crude product from methanol yielded yellow needle crystals (16.5 g). Yield: 47%. Anal. Calcd for $C_{17}H_{15}N_1O_5$: C, 65.17; H, 4.83; N, 4.47. Found: C, 64.95; H, 4.92; N, 4.42. ^{1}H NMR (270 MHz, $CDCl_3$): δ 1.52 (t, J=8.1 Hz, 3H, CH_3), 4.52 (q, J=8.1 Hz, 2H, CH_2), 7.02−6.93 (m, 2H, ph), 7.49 (t, J=7.0 Hz, 1H, py), 7.69 (s, 1H), 8.19−7.95 (m, 2H, ph), 8.27−8.20 (m, 2H, py), 12.07 (s, 1H, OH), 15.15 (s, 1H, OH). **H_2L2:** Hydrazine monohydrate (3.5 g, 70 mmol) was added to an ethanolic solution of 6-[1,3-dioxo-3-(2-hydroxyphenyl)propionyl]pyridine-2-carboxylic acid ethyl ester (20.0 g, 63 mmol), and the mixture was refluxed for 1 h. The resulting mixture was evaporated and allowed to stand for several hours at 5 °C to yield colorless needles (11.88 g, 38 mmol). Yield: 61%. Anal. Calcd for $C_{17}H_{15}N_3O_3\cdot 0.5H_2O$: C, 64.14; H, 5.04; N, 13.20. Found: C, 64.46; H, 5.19; N, 13.28. ^{1}H NMR (270 MHz, $CDCl_3$): δ 1.47 (t, J=7.2 Hz, 3H, CH_3), 4.49 (q, J=7.2 Hz, 2H, CH_2), 6.94 (t, J=7.4 Hz, 1H, ph), 7.06 (t, J=8.1 Hz, 2H, ph), 7.27−7.21 (m, 1H, ph), 7.63−7.60 (m, 1H, pz), 8.08−7.84 (m, 3H, py), 12.10 (s, 1H, OH), 10.80 (s, 1H, NH).

(8) Synthesis of **1**: A solution of $Mn(OAc)_2\cdot 4H_2O$ (49 mg, 0.2 mmol) in methanol (5 mL) was added to the mixture of H_2L2 (62 mg, 0.2 mmol) and triethylamine (56 μL, 0.4 mmol) in methanol (5 mL). Chloroform (10 cm^3) was added to the resulting solution. After the solution was stirred for several minutes, NEt_4BF_4 (22 mg, 0.1 mmol) was added, and the resulting solution was refluxed for 10 min before hot filtration. The filtrate was allowed to cool to room temperature and stand for a few days to give brown plate crystals of **1**. Anal. Calcd for $C_{68}H_{56}Mn_4N_{12}O_{16}$: C, 52.27; H, 3.94; N, 10.76. Found: C, 50.67; H, 3.76; N, 10.36. Synthesis of **2**: A mixed solution of $Mn(OAc)_2\cdot 4H_2O$ (24.5 mg, 0.1 mmol) in methanol (3 mL) and bis(pentamethylcyclopentadienyl)iron (32.6 mg, 0.1mmol) in chloroform (3 mL) was added to the mixture of H_2L2 (62 mg, 0.2 mmol) and triethylamine (112 μL, 0.8 mmol) in methanol (4 cm^3). The mixture was stirred for several minutes. NH_4PF_6 (163 mg, 1.0 mmol) was added to the mixture, and the resulting solution was filtered. The filtrate was allowed to stand for a few days at room temperature to give brown rhombic plate crystals of **2**. Anal. Calcd for $C_{68}H_{59}F_{12}Mn_4N_{12}O_{16.5}P_2$: C, 44.91; H, 3.27; N, 9.25. Found: C, 45.66; H, 3.49; N, 9.61.

(9) Crystal data for **1**: brown plate crystals (0.30 × 0.20 × 0.05 mm^3), $C_{68}H_{61}Mn_4N_{12}O_{18.5}$, M=1562.03, orthorhombic, *Pnnn*, a=20.135(2) Å, b=20.145(2) Å, c=17.2055(18) Å, V=6978.8(12) $Å^3$, Z=4, d_{calcd}=1.459 mg m^{-3}, μ(Mo Kα)=0.784 mm^{-1}, T=100 K. A total of 35 094 were collected (4.74° < θ < 48.58°) of which 6328 unique reflections (R_{int}=0.0487) were measured. R1=0.0713, wR2=0.2068 ($I > 2\sigma$), and S=1.055. Crystal data for **2**: brown rhombic plates (0.42 × 0.25 × 0.04 mm^3), $C_{70}H_{64}Cl_3F_{12}Mn_4N_{12}O_{16.5}P_2$, M = 1949.34, triclinic, $P\bar{1}$, a = 16.063(3) Å, b = 16.722(3) Å, c = 17.021(3) Å, α=76.977(3)°, β=73.151(3)°, γ=70.571(3)°, V=4084.3(13) $Å^3$, Z=2, d_{calcd}=1.563 mg m^{-3}, μ(Mo Kα)=0.839 mm^{-1}, T=200 K. A total of 16 607 were collected (4.16° < θ < 46.56°) of which 11 393 unique reflections (R_{int}=0.0265) were measured. R1=0.0641, wR2=0.1653 ($I > 2\sigma$), and S=0.926. Both data sets were treated with the SQUEEZE program to deal with disordered solvent molecules, The crystallographic formulas have been amended to include the number of solvent molecules suggested by SQUEEZE (see the CIF files).

(10) BVS of **1**: Mn1 for +3, 3.001; Mn2 for +3, 3.001.

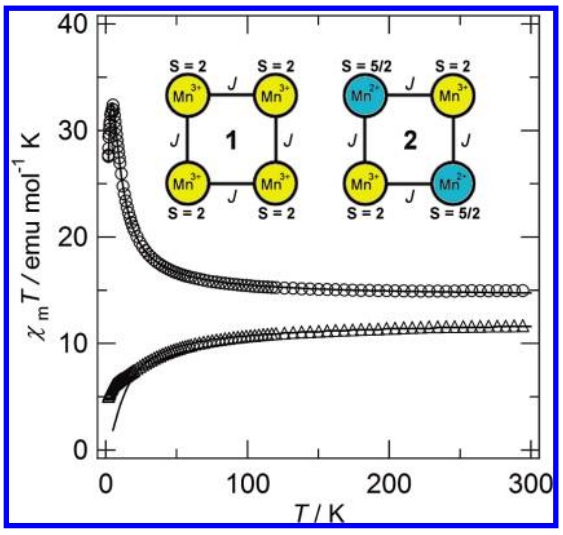

Figure 2. $\chi_m T$ vs T plots of **1** (△) and **2** (○). Solid lines are theoretical curves (see the text). Inset: spin states of each complex and magnetic exchange paths.

coordinated keto oxygen atoms from the ethyl ester groups with an average Mn−O distance of 2.506 Å. The bond lengths, observed Jahn−Teller distortions, and BVS calculations[11] suggest that Mn1 and Mn3 are trivalent and Mn2 and Mn4 are divalent. Both complexes have tetranuclear square-like metal arrangements, but the arrangements of metal ions in **1** and **2** are square and rhombic, respectively. The manganese centers in **1** are all bridged by pyrazole groups and methoxo ions, whereas in **2**, the manganese ions are only bridged by pyrazole groups. Both **1** and **2** have gridlike structures derived from similar components, four manganese ions and four asymmetric ligands; however, both showed very different magnetic behavior. Magnetic susceptibility measurements were collected for **1** and **2** in the temperature range of 1.8−300 K in an applied field of 500 Oe (Figure 2). For **1**, the $\chi_m T$ value of 10.99 emu mol^{-1} K at 300 K is smaller than the expected value (12.00 emu mol^{-1} K) for four magnetically uncorrelated Mn^{III} ions ($S = 2$; $g = 2$). As the temperature decreased, the $\chi_m T$ value gradually decreased, reaching a minimum value of 5.21 emu mol^{-1} K at 1.8 K. For **2**, the $\chi_m T$ value of 14.87 emu mol^{-1} K at 300 K is slightly larger than the value (14.75 emu mol^{-1} K) expected for two magnetically uncorrelated Mn^{III} ions ($S = 2$; $g = 2$) and two Mn^{II} ions ($S = {}^5/_2$; $g = 2$). As the temperature decreased, the $\chi_m T$ value gradually increased, reaching a maximum value of 32.40 emu mol^{-1} K at 5.0 K, followed by a sudden decrease. In addition to this ferromagnetic behavior, **2** also showed a limited degree of alternating-current susceptibility, suggesting superparamagnetic properties (Figure S2 in the Supporting Information). These magnetic data were fitted to isotropic exchange Hamiltonians (see the Supporting Information). It should be noted that the exchange coupling constants between neighboring manganese ions are treated as being identical for all four bridges in **1** and **2**, respectively, because the same bridging modes are active between all metal centers in each cluster. Fitting of the experimental data gave $g = 1.94$ and $J = -1.29$ K for **1** and $g = 1.97$, $J = +0.84$ K, $D_{fixed} = -0.22$ K, and $zJ' = -1.74$ K for **2**, where J represents the exchange coupling constant between neighboring manganese ions (Figure 2, inset).[12] The observed J value for **1** is in a range similar to that of previously reported Mn^{III}−NN−Mn^{III}/Mn^{III}−O−Mn^{III} interaction pathways;[13] however, there are no known examples of Mn^{III}−NN−Mn^{II} mixed-valence interaction pathways to allow an effective comparison with **2**. To explain the antiferromagnetic interactions of **1**, there are two exchange pathways that must be considered: the methoxo bridge, which occupies the d_{z^2} orbital of one Mn^{III} center and the $d_{x^2-y^2}$ orbital of the next, and the pyrazole bridges, which link the $d_{x^2-y^2}$ orbitals of neighboring Mn^{III} centers. Because the $d_{x^2-y^2}$ orbitals are unoccupied in Mn^{III}, the pyrazole bridge leads to negligible magnetic interaction; however, the methoxo bridge would be expected to lead to ferromagnetic interactions because of the orthogonality of the interacting d_{z^2} and $d_{x^2-y^2}$ orbitals. The antiferromagnetic nature of the cluster may be due to the large Mn−O−Mn angles [118.08(16)−118.09(16)°], which may lead to mixing of the orbitals and interaction between the d_{z^2} orbital and the d_{xy} orbital of the neighbor. In the case of **2**, the Mn^{III} ions with square-pyramidal coordination geometry (Mn1 and Mn3) have their Jahn−Teller axes filled by coordinated water molecules. Note that each Mn^{III} ion has a vacant $d_{x^2-y^2}$ orbital that is oriented toward the bridging pyrazole groups. These groups constitute the path for the magnetic interaction between the Mn^{III} and Mn^{II} centers, so as a result the interacting spin of the Mn^{II} ions may be partially delocalized to the vacant $d_{x^2-y^2}$ orbital of the Mn^{III} ions, causing the occurrence of intramolecular ferromagnetic interactions.

In conclusion, two tetranuclear manganese gridlike complexes were synthesized using a rigid multidentate asymmetric ligand. **1** has four antiferromagnetically coupled Mn^{III} ions, while **2** consists of two divalent and two trivalent manganese ions, all of which are ferromagnetically coupled.

Acknowledgment. This work was supported by a Grant-in-Aid for Scientific Research and for Priority Area "Coordination Programming" (area 2107) from MEXT, Japan.

Supporting Information Available: Additional magnetic data, isotropic exchange Hamiltonians, and crystallographic data in CIF format. This material is available free of charge via the Internet at http://pubs.acs.org.

(11) BVS of **2**: Mn1 and Mn3 for +3, 3.171 and 3.196, respectively; Mn2 and Mn4 for +2, 1.843 and 1.817, respectively.

(12) The D value was estimated from the magnetization data at 1.8 K (Figure S3 in the Supporting Information), and the exchange coupling constant was then obtained by analyzing the magnetic susceptibility data with a fixed D value. TIP(**1**) = 400 × 10^{-6} emu mol^{-1}, and TIP(**2**) = 200 × 10^{-6} emu mol^{-1}.

(13) Stoicescu, L.; Jeanson, A.; Duhayon, C.; Tesouro-Vallina, A.; Boudalis, A. K.; Costes, J.-P.; Tuchagues, J.-P. *Inorg. Chem.* **2007**, *46*, 6902.